Numerical study on the characteristics of nitrogen discharge at high pressure with induced plasma*

Wang Yi-Nan(王一男), Liu Yue(刘 悦)†,
Zheng Shu(郑 殊), and Lin Guo-Qiang(林国强)

Key Laboratory of Materials Modification by Laser Ion and Electron Beams, Dalian University of Technology, Dalian 116024, China

(Received 9 November 2011; revised manuscript received 9 February 2012)

Based on the fluid theory of plasma, a model is built to study the characteristics of nitrogen discharge at high pressure with induced argon plasma. In the model, species such as electrons, N_2^+, N_4^+, Ar^+, and two metastable states ($N_2(A^3\sum_u^+)$, $N_2(a^1\sum_u^-)$) are taken into account. The model includes the particle continuity equation, the electron energy balance equation, and Poisson扭equation. The model is solved with a finite difference method. The numerical results are obtained and used to investigate the effect of time taken to add nitrogen gas and initially-induced argon plasma pressure. It is found that lower speeds of adding the nitrogen gas and varying the gas pressure can induce higher plasma density, and inversely lower electron temperature. At high-pressure discharge, the electron density increases when the proportion of nitrogen component is below 40%, while the electron density will keep constant as the nitrogen component further increases. It is also shown that with the increase of initially-induced argon plasma pressure, the density of charged particles increases, and the electron temperature as well as the electric field decreases.

Keywords: induced plasma, nitrogen discharge, numerical simulation

PACS: 52.65.–y, 52.80.Pi, 52.77.Fv **DOI:** 10.1088/1674-1056/21/7/075202

1. Introduction

Gas discharges are widely used in such various fields as etching and deposition of films,[1,2] surface treatment,[3] ozone generation,[4] bio-sterilization,[5] fusion,[6] and thrusters. [7] Currently, most of the plasma sources are operated at low pressures for the sake of the facility to generate a large-area, uniform glow discharge plasma. The cold plasma is highly nonequilibrium in that the electron temperature is much higher than that of ions and neutral species. However, the low-pressure discharge yields low-density plasmas. Compared with the plasma sources originating from a low-pressure discharge, the plasmas from a high-pressure discharge show outstanding features, especially for high-density plasmas. Traditional high-pressure discharges usually rely on techniques that avoid the instabilities which develop a glow-to-arc transition. Only if the current density remains below the threshold of the glow-to-arc transition, it is possible to generate a stable glow discharge at both high (up to atmospheric pressure) and low pressures (< 10 Torr).[8−10] As an alternative technique for generating steady-state plasmas from a high-pressure discharge, using dielectric barrier covered electrodes has been reported in the last decade.[11−14] The dielectric barrier can be considered as a capacitor in series with a gas gap and its charge limits the voltage applied to the gas avoiding the instability.[15] Another approach has been put forward to operate a high-pressure discharge in the pulsed discharge with current densities that exceed the threshold but the duration of the discharge pulse is chosen to be shorter than the time scales for causing instability.[16−18] Other approaches have also been proposed, such as microwave-driven large-volume high-pressure discharge.[19]

Recently, a kind of radiofrequency (RF) atmospheric-pressure glow discharge plasma of air, nitrogen, and oxygen operating steadily in a γ mode based on an induced gas discharge approach was reported by Li and co-authors.[20,21] They show that for a glow discharge plasma operating in α mode, the gas ionization occurs throughout the electrode gap, driven mainly by the oscillatory field of the applied voltage; while operating in γ mode, the gas ionization is localized near the boundary between the sheath and the plasma bulk, largely driven by significant secondary electrons after

*Project supported by the National Science Foundation of China (Grant No. 10675029), the National Basic Research Program of China (Grant Nos. 2008CB717801, 2008CB787103, 2009GB105004, and 2010GB106002), and FRFCU (Grant No. DUT12ZD201).

†Corresponding author. E-mail: liuyue@dlut.edu.cn

© 2012 Chinese Physical Society and IOP Publishing Ltd

a breakdown with the plasma-induced gas (e.g., helium or argon), and then the discharge mode is transferred to the γ mode by adjusting the operating parameters. At last, the flow rate of the plasma-formed gas (e.g., air, nitrogen, and oxygen) is increased to generate the γ mode discharge with a plasma-induced gas mixture, and a stable glow discharge plasma operating in γ mode is obtained by decreasing the plasma-induced gas flow rate. This approach can succeed in generating cheap gas glow discharge plasma at atmospheric pressure. Yu *et al.* numerically studied the characteristics of argon RF glow discharge plasma at high pressure using a similar method.[22] In their work, the gas pressure is increased up to 100 Torr. Subsequent to generating induced plasma at low pressure, a stable glow argon discharge is operated at high pressure.

In this paper, a similar concept to the induced argon plasma approach for producing RF high pressure discharge with nitrogen as working gas is described in detail. This method makes the requirement of a stable nitrogen discharge at high pressure relatively easy to realize. It can be described in brief as follows: first, generating an argon plasma at a low pressure of 1 Torr; secondly, adding a nitrogen gas into the argon plasma at a pressure up to 200 Torr; and at last, a stable argon-nitrogen mixture gas discharge is operated at high pressure. Obviously, there are some differences between our method and those proposed by Li *et al.* and Yu *et al.* A fluid model is built and solved numerically to describe this process. The influence of the time the nitrogen gas is added to the induced argon plasma and the pressure of the induced argon plasma are also discussed in this paper. The numerical results show that a nitrogen discharge with induced plasma in high pressure in this work can be operated to obtain high-density plasma at low conditions compared with a pure nitrogen discharge.

2. Model

To study the characteristics of nitrogen discharge with induced argon plasma, a fluid model was used for describing the plasma discharge. A schematic of the discharge system is shown in Fig. 1 in Ref. [23], where the right electrode is powered from RF voltage and the left electrode is grounded. The electrode gap is set to be 2.0 cm, the peak voltage is 300 V, and the frequency of RF is 13.56 MHz. Since there are multi-excited-state nitrogen molecules, we must simplify the model in our simulation. In our model, we consider the particle species: e, N_2^+, N_4^+, Ar^+, and two low-energy metastable states $N_2(A^3\sum_u^+)$ and $N_2(a^1\sum_u^-)$. For simplicity, $N_2(A^3\sum_u^+)$ and $N_2(a^1\sum_u^-)$ are written as $N_2(A)$ and $N_2(a)$, respectively.

The main reactions are presented in Table 1. The basic assumptions of the model are listed as follows:

1) Since the electrode area is large and the parallel plate radius is much greater than electrode gap, we assume that the discharge properties change along the direction perpendicular to the electrodes (only the x axis).

2) The charged particle flux is described by the drift/diffusion approximation.

3) The electron-energy distribution function is assumed to be Maxwellian.

4) The temperatures of ions and neutral species are assumed to equal the gas temperature.

Table 1. Important collision processes in argon and nitrogen discharge.

No.	Reaction	Rate coefficient/$cm^3{\cdot}s^{-1}$	Ref.
1	$e + Ar \rightarrow Ar^+ + 2e$	$k = \begin{cases} 0, & T_e \le 5.3 \\ 8.7\times10^{-9}(T_e-5.3)\exp(-4.9/\sqrt{T_e-5.3}), & T_e > 5.3 \end{cases}$	[22]
2	$e + N_2 \rightarrow N_2^+ + 2e$	$k = 5.9\times10^{-9}T_e^{0.917}\exp(-15.6/T_e)$	[24]
3	$e + N_2 \rightarrow N_2(A) + e$	$k = 4.05\times10^{-9}\exp(-5.36/T_e)$	[24]
4	$e + N_2 \rightarrow N_2(a) + e$	$k = 1.47\times10^{-9}\exp(-8.79/T_e)$	[24]
5	$N_2(a) + N_2(A) \rightarrow N_4^+ + e$	$k = 5\times10^{-11}$	[24]
6	$N_2(a) + N_2(a) \rightarrow N_4^+ + e$	$k = 2\times10^{-10}$	[24]
7	$N_2(a) + N_2 \rightarrow N_2(B) + N_2$	$k = 3\times10^{-16}$	[24]
8	$N_2(A) + N_2 \rightarrow N_2 + N_2$	$k = 1.9\times10^{-13}$	[24]
9	$e + N_2^+ \rightarrow N + N$	$k = 4.8\times10^{-7}(300/T_e)^{0.5}$	[25]
10	$N_2 + N_4^+ \rightarrow 2N_2 + N_2^+$	$k = 2.1\times10^{-16}\exp(T_g/121)$	[24]
11[a)]	$2N_2 + N_2^+ \rightarrow N_2 + N_4^+$	$k = 6.8\times10^{-29}\exp(300/T_g)^{1.64}$	[24]
12	$N_2(A) + N_2(A) \rightarrow N_2(B) + N_2$	$k = 7.7\times10^{-11}$	[24]
13	$Ar^+ + N_2 \rightarrow N_2^+ + Ar$	$k = 4.45\times10^{-10}$	[25]
14	$Ar + N_2^+ \rightarrow N_2 + Ar^+$	$k = 2.81\times10^{-10}$	[25]

[a)] Rate coefficient (in units of cm^6) for reaction 11. T_e is the electron temperature (in eV), and T_g is the gas temperature (in K).

The continuity equations for particles can be written as

$$\frac{\partial n_{\rm e}}{\partial t} + \boldsymbol{\nabla}\cdot\boldsymbol{J}_{\rm e} = S_{\rm e}, \tag{1}$$

$$\frac{\partial n_{\rm i}}{\partial t} + \boldsymbol{\nabla}\cdot\boldsymbol{J}_{\rm i} = S_{\rm i}, \tag{2}$$

$$\frac{\partial n_{*}}{\partial t} + \boldsymbol{\nabla}\cdot\boldsymbol{J}_{*} = S_{*}. \tag{3}$$

The particle fluxes under the drift/diffusion approximation are expressed as

$$\boldsymbol{J}_{\rm e} = -\mu_{\rm e} n_{\rm e}\boldsymbol{E} - D_{\rm e}\boldsymbol{\nabla} n_{\rm e}, \tag{4}$$

$$\boldsymbol{J}_{\rm i} = \mu_{\rm i} n_{\rm i}\boldsymbol{E} - D_{\rm i}\boldsymbol{\nabla} n_{\rm i}, \tag{5}$$

$$\boldsymbol{J}_{*} = -D_{*}\boldsymbol{\nabla} n_{*}. \tag{6}$$

The electron-energy balance can be expressed as

$$\frac{\partial}{\partial t}\left(\frac{3}{2}n_{\rm e}kT_{\rm e}\right) = -\boldsymbol{\nabla}\cdot\boldsymbol{q}_{\rm e} - e\boldsymbol{E}\Gamma_{\rm e} - \sum_j H_j R_j, \tag{7}$$

with the total electron-energy flux being

$$\boldsymbol{q}_{\rm e} = -\frac{5}{2}D_{\rm e}n_{\rm e}\boldsymbol{\nabla}T_{\rm e} + \frac{5}{2}kT_{\rm e}\Gamma_{\rm e}. \tag{8}$$

Finally, the Poisson equation reads

$$\frac{\partial^2 V}{\partial x^2} = -\frac{e}{\varepsilon_0}\left(\sum_j n_{{\rm i}j} - n_{\rm e}\right). \tag{9}$$

From the potential, we can derive the electric field as

$$\boldsymbol{E} = -\boldsymbol{\nabla}V. \tag{10}$$

In Eqs. (1)–(9), n_l, J_l, D_l, and μ_l ($l = {\rm e}, +, *$) are the densities of species, flux, diffusion coefficient, and mobility, respectively. The parameters D_l and μ_l can be found in Refs. [21] and [22]. The parameter $S_{\rm e,i,*}$ denotes the source term. The subscripts $({\rm e}, +, *)$ represent electrons, positive ions, and metastable molecules, respectively. In addition, k is the Boltzmann coefficient, $T_{\rm e}$ is the electron temperature, $q_{\rm e}$ is the conductive heat flux, e, ε_0, and V are the element charge, the permittivity of free space, and the potential, respectively.

It is assumed that the densities of species at the electrode are zero. The electron temperature is a constant of 0.5 eV at the electrodes. The voltage used in the simulation is a sinusoidal wave form and this form on the driven electrode is $V = V_{\rm p}\sin(2\pi f t)$, where $V_{\rm p}$ is the peak voltage, and f is the ac frequency. The other electrode is grounded.

The initial particle densities at low pressure are small, $n_{\rm e} = n_{\rm Ar^+} = 10^7$ cm^{-3}. Tests under different initial conditions show that the little influence of the final low-pressure glow discharge is the key point in previous publications.[23,26] This system of equations were discretized in space by using the center difference of an interlaced grid, and in time by using an implicit scheme. The matrix equations were obtained by discretizing and solved by a chase-after method.

3. Results and discussion

First, for the induced argon gas discharge at 1 Torr, we numerically calculate the distributions of electron density, argon ion density, electron temperature, electric field, and voltage. Using these results as the initial conditions, we numerically solve the model of the nitrogen discharge when adding nitrogen gas into the induced argon plasma from 1 to 200 Torr.

The numerical results are shown in Fig. 1, where the stable distributions of particle density and electron temperature in space at 200 Torr are presented. It can be clearly seen that the N_4^+ density is higher than the other ions. It is three or four orders higher than that of N_2^+, which is in the same order as Ar^+. The peaks of Ar^+ density and N_2^+ density are near the right electrode, where the electron density is smaller than in the bulk plasma. The curve of N_2^+ is similar to that of Ar^+. Because the pathways of electrons and N_2^+ ions are fast in the reactions, when the electron density is high, the density of N_2^+ ions will decrease by this loss mechanism. In Fig. 1, it is evident that the electron curve overlaps with the N_4^+ curve in the bulk plasma. The electron temperature is nearly a constant of 5.4 eV in bulk plasma and it is much smaller than that in the sheath. In this work, due to the presence of the induced argon plasma, the electron temperature increases to 5.4 eV in

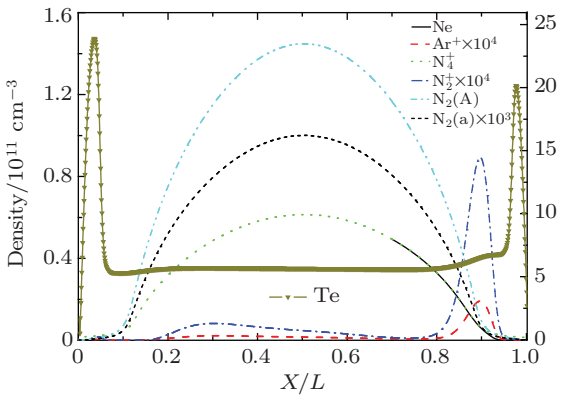


Fig. 1. (colour online) Distributions of particle density under the following conditions: an induced argon gas pressure of 1 Torr, a final mixture-gas pressure of 200 Torr, the time when nitrogen gas was added is 0.1106 ms.

the bulk region. As time goes, the electron temperature is always greater than 5.3 eV in the bulk region. The argon ionization coefficient implies that there is no appreciable ionization for an electron temperature below 5.3 eV. When the electron temperature is greater than 5.3 eV, argon ionization occurs and produces electron seeds to maintain the gas ionization in high pressure. Therefore, the nitrogen discharge with induced argon plasma can raise the electron temperature and create nitrogen plasmas in high pressure under these conditions.

Based on the comparison between the results under different conditions, i.e., with and without induced argon plasma, as shown in Table 2, it can be seen that the nitrogen discharge with induced plasma in high pressure in this work can be operated at low conditions, such as a comparatively small applied voltage, high pressure, and large gap. Moreover, it can create relatively high-density plasma.

Table 2. Comparison between the results under different conditions, i.e., with and without an induced argon plasma in nitrogen discharge.

Voltage/V	Current/mA	Gap/cm	Pressure/Torr
300	–	2.3[a)]	200[a)]
8500	–	0.2[b)]	760[b)]
–	10[c)]	3.2[c)]	3.9[c)]

[a)]With induced argon plasma, [b)]without induced argon plasma 1 (Ref. [27]), [c)]without induced argon plasma 2 (Ref. [28]).

In this paper, we also discuss the effects of the time when the nitrogen gas is added and initial argon plasma pressure P_0 on the nitrogen discharge. The initial induced argon plasma pressure increases from P_0 (0.5–2 Torr) to P_b (200 Torr). As mentioned above, the number of N_4^+ ions is much greater than N_2^+ and Ar^+ in Fig. 1. In what follows, the electron density, N_4^+ density, electron temperature, and electric field are discussed in detail.

3.1. Effect of the time when the nitrogen gas is added on the nitrogen discharge

The influence of the time the nitrogen gas is added is investigated. The initial induced argon plasma pressure is 1 Torr. Here we assume that the variation of gas pressure is linear with time. That is, $P(t) = (P_b - P_0)T^{-1}t + P_0$, where T is the time of adding the nitrogen gas and $P(t)$ is the pressure of the mixture gas. We calculate the discharge when the nitrogen gas is added at different times. Because the rate of varying gas pressure equals $(P_b - P_0)/T$, a longer time indicates a lower rate of varying gas pressure.

From Fig. 2(a), it can be seen that the electron density increases with increasing T. Figure 2(b) shows the distribution of N_4^+ density when the nitrogen gas is added at different times. It can be seen that the N_4^+ density increases with T, and has the same trend as the electron density. Figures 2(a) and 2(b) also provide the electron density and N_4^+ density at the middle point between the electrodes with different T. It can be clearly seen that both of these densities increases with T. When the time nitrogen gas is added is less than 0.06 ms, the charged particle densities increase quickly. However, when the time nitrogen gas is added is more than 0.06 ms, the charged particle densities almost remain unchanged.

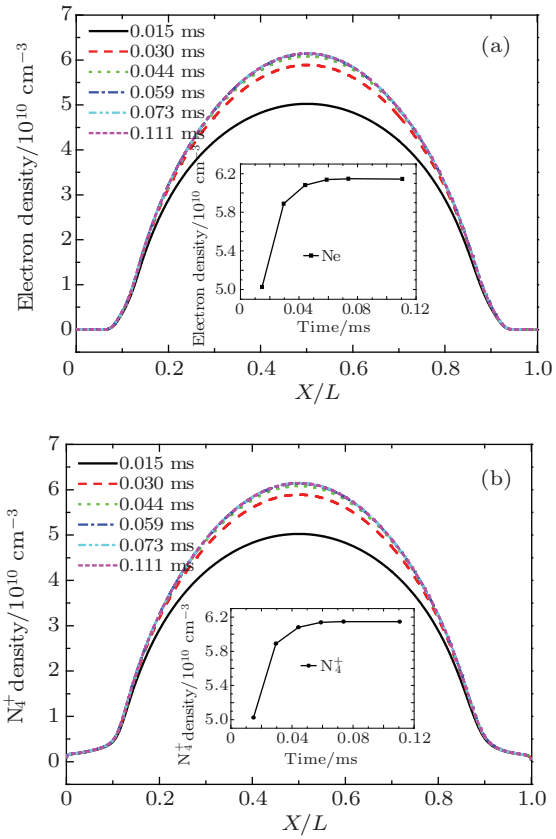


Fig. 2. (colour online) (a) Electron density distribution and (b) N_4^+ density distribution when nitrogen gas is added at different times.

The electron temperature and electric field at different T are plotted in Fig. 3. It can be seen that the electron temperature and electric field have a small variation with T. In order to see more clearly, the electron temperature and electric field at the middle point between the electrodes at different T are also

given. It is shown in Fig. 3(a) that the electron temperature at the middle point between the electrodes decreases with increasing time. When the time nitrogen gas is added is less than 0.06 ms, the electron density increases quickly and the electron temperature also decreases quickly. When the time the nitrogen gas is added is more than 0.06 ms, the electron density is nearly kept constant and the electron temperature is also nearly kept constant. The electron temperature has an opposite variation to the electron density. From Fig. 3(b), we can see that the electric field almost decreases with increasing T. However, when the time nitrogen gasis added is above 0.06 ms, the electric field does not remain constant like the electron temperature.

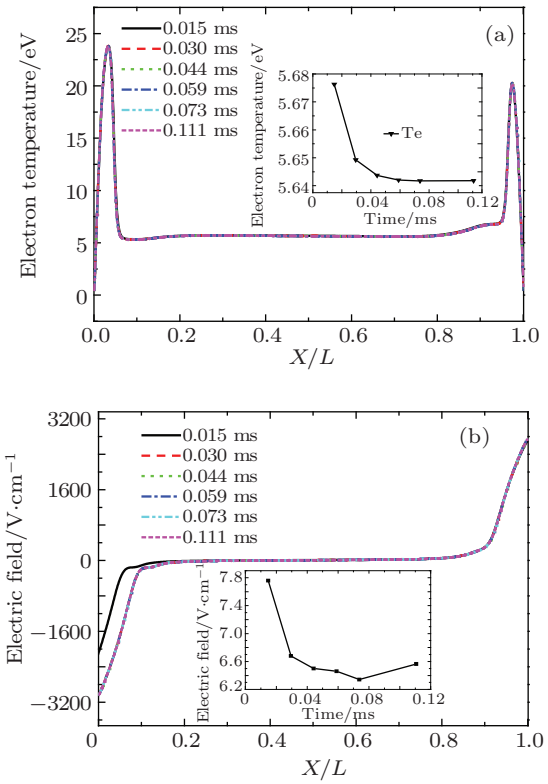


Fig. 3. (colour online) (a) Electron temperature distribution and (b) electric field distribution for different velocities of adding nitrogen gas.

The above-mentioned results indicate that a high rate of varying gas pressure results in short time of species reactions, and the reactions among species are not sufficient. The long time of adding nitrogen gas can make the reactions between particles sufficient. Thus, the densities of electron and N_4^+ increase with increasing time of adding the nitrogen gas. The electrons gain energy from the electric field. When the electric field decreases with T, the electron temperature also decreases. In Ref. [21], it is stated that a lower rate of varying gas pressure leads to a higher electron density. The results of the effect of the time nitrogen gas is added are in agreement with that in Ref. [21].

3.2. Effect of the initial induced argon plasma pressure P_0 on the nitrogen discharge

Figure 4 shows the charged species density distribution at different induced argon plasma pressures P_0 (0.5–2 Torr). The time nitrogen gas was added is 0.11 ms. We can see that the electron density and N_4^+ density increase with increasing P_0, and they almost have the same value in the plasma, which satisfies charge neutrality. Since the electron density increases with P_0, the reactions of e + N_2 → N_2(A) + e and e + N_2 → N_2(a) + e are enhanced, and thus the densities of N_2(A) and N_2(a) increase. For the processes of N_2(A) + N_2(a) → N_4^+ + e and N_2(a) + N_2(a) → N_4^+ + e, these reactions are enhanced to produce electrons. It is a positive feedback process to produce more electrons. Since the induced argon plasma exists, the inelastic collisions between electrons and neutral gas are enhanced.

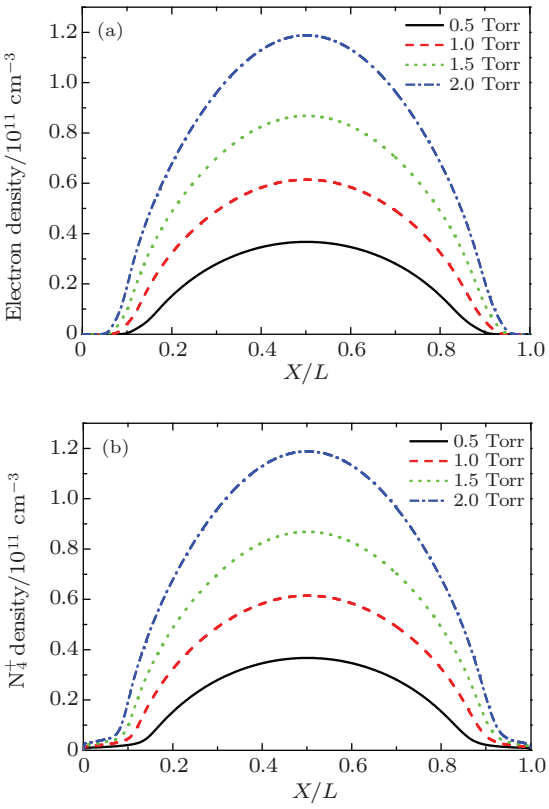


Fig. 4. (colour online) (a) Electron density distribution and (b) N_4^+ density distribution for different initial argon plasma pressure P_0.

At high pressure, it is shown in Fig. 5 that with as nitrogen gas is added to the argon plasma, the electron density increases when the constituent of the nitrogen gas exceeds 40%. This is different from a low-pressure argon–nitrogen gas discharge. Gao *et al.* have reported that in RF inductively coupled Ar–N_2 plasma, the electron density drops substantially at a pressure above 1.3 Pa when a small amount of N_2 is added to the gas mixture because of the dissociative recombination of electrons and argon ions or nitrogen ions.[26] In our model, we neglect the reaction of electrons and argon ions. However, the dissociative recombination of electrons and N_2^+ ions is taken into account. The mechanisms of the increase of the electron density due to nitrogen addition are associative ionization processes, and these processes reverse the dissociative recombination of electrons and N_2^+ ions. The electron density with nitrogen addition profiles shows significant differences from Ref. [26] due to different mechanisms of generating electrons. The larger induced argon plasma pressure in the low-pressure glow discharge can provide more active species for the high-pressure nitrogen glow discharge.

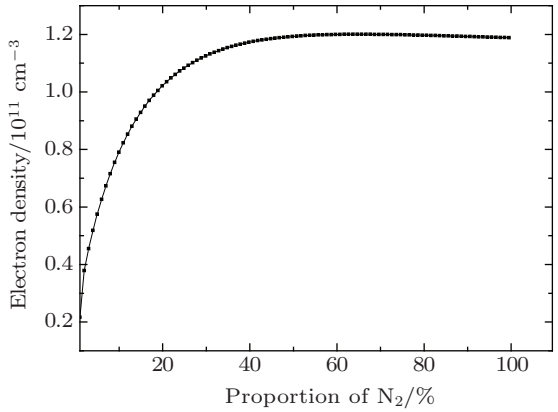


Fig. 5. Maximum electron density under different proportions of nitrogen gas.

Figure 6 presents the electron temperature and electric field under different induced argon plasma pressures. In Fig. 6(a), the electron temperature decreases with the initial induced argon plasma pressure P_0. In the bulk plasma, the electron temperature decreases from 5.67 to 5.22 eV. As the electron density increases, the electron-impact ionizations of neutral atoms and molecules increase, and the increase of loss energy term $\sum_j H_{i,j} k_{i,j} n_e N$ is faster than that of the Ohmic heating term $eE\Gamma_e$. We can also see that the sheath thickness decreases with the increase of the initial induced argon plasma pressure. It can also be seen in Fig. 6(b) that electric field is between electrodes. The sheath region decreases and the bulk plasma region increases. Therefore, more particles are bonded into the bulk plasma and more particles participate in the reactions.

Our results show that the density of plasma increases with the increase of the initial induced argon plasma pressure from 0.5 to 2 Torr. With the increase of the initial induced argon plasma pressure, the electron seeds increase, and the collision frequency among electrons and argon atoms increases. More ionization occurs and the plasma density increases. The induced argon plasma pressure provides active species for nitrogen discharge, and a higher induced argon plasma pressure can provide more active species. In our results, the RF induced plasma discharge can produce more plasma, whose density is about 10^{11} cm^{-3}. Comparison with available experimental data suggests that the plasma density obtained in this work is higher than that reported in Ref. [29].

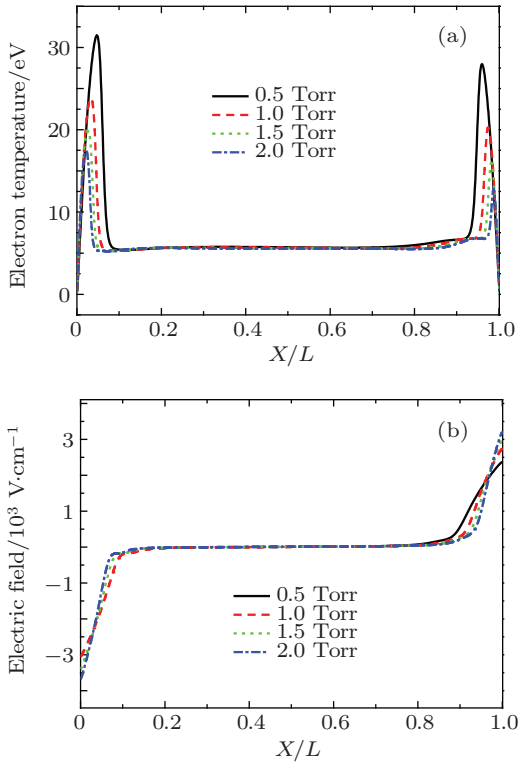


Fig. 6. (colour online) (a) Electron temperature distribution and (b) electric field distribution at different initial argon plasma pressure P_0.

4. Conclusions

A numerical model is adopted to simulate the nitrogen discharge at high pressure with argon induced plasma. The numerical results are obtained from the model. Through analyzing the results, it is found that,

firstly, the induced argon plasma can provide high-energy electrons and it is favorable to ionize the gas. It also can support high electron temperatures and produce nitrogen plasma at high pressure when the applied voltage is relatively low. Secondly, the electron density and N_4^+ density increase with the increase in the time the nitrogen gas is added, the electron temperature and the electric field decrease under the same conditions. Finally, with the increase of the initial induced argon plasma pressure, the charged particles increase, and the electron temperature and electric field decrease. Since the initial induced argon plasma pressure can provide active species for nitrogen discharge, and a higher induced argon plasma pressure will provide more active species, it is concluded that high-density plasma can be obtained with this method, in which the induced gas discharge is used under low pressure and then the pressure is increased to some extent.

References

[1] Corbella C, Rubio-Roy M, Bertran E and Andújar J L 2009 *J. Appl. Phys.* **106** 033302

[2] Goto H H, Lowe H D and Ohmi T 1993 *IEEE Trans. Semicond. Manuf.* **6** 58

[3] Lieberman M A and Lichtenberg A J 2005 *Principles of Plasma Discharges and Materials Processing* (NewYork: Wiley-Interscience) p. 1 (in Chinese)

[4] Kogoma M and Okazaki S 1994 *J. Phys.* D **24** 1985

[5] Ding L L, Xu L, Zhang R, Liu P and Zhan R J 2004 *Chin. Phys.* **13** 0913

[6] Sheng Z M, Mima K, Senloku Y, Jovanović M S, Taguchi T, Zhang J and Meyer-ter-Vehn J 2002 *Phys. Rev. Lett.* **88** 055004

[7] J Yang, He H Q, Mao G W and Shi S L 1998 *J. Propulsion Technol.* **19** 21 (in Chinese)

[8] Suits C G 1939 *J. Appl. Phys.***10** 648

[9] Gambling W A and Edels H 1953 *J. Appl. Phys.* **5** 36

[10] Haas R A 1973 *Phys. Rev.* A **8** 1017

[11] Geng Y M, Lu C H, Liang M and Zhang W 2010 *Plasma Sci. Technol.* **12** 715

[12] Dong L F, Mao Z G and Ran J X 2005 *Chin. Phys.* **14** 1618

[13] Zhu X M and Kong M G 2005 *J. Appl. Phys.* **97** 083301

[14] Shang W L, Wang D Z and Zhang Y T 2008 *Phys. Plasmas* **15** 093003

[15] Massines F, Segur P, Gherardi N, Khamphan C and Ricard A 2003 *Surf. Coat. Tech.* **174** 8

[16] Walsh J L, Shi J J and Kong M G 2006 *Appl. Phys. Lett.* **88** 17150

[17] Yang W D, Wang P N, Liu Z P, Mi L and Li F M 2002 *Chin. Phys.* **11** 0260

[18] Shi J J, Ca Y Q, Zhang J, Ding K and Zhang J 2009 *Phys. Plasmas* **16** 070702

[19] Li H P, Sun W T, Wang H B, Li G and Bao C Y 2007 *Plasma Chem. Plasma P.* **27** 529

[20] Li H P, Li G, Wang S, Le P S and Bao C Y 2008 *IEEE Trans. Plasma Sci.* **36** 4

[21] Yu Q, Deng Y F, Liu Y and Han W X 2008 *Chin. Phys. Lett.* **25** 2569

[22] Dimitris P L and Demetre J E 1993 *J. Appl. Phys.* **73** 3668

[23] You Z W 2009 *The Fluid simulation of N2-O2 Dual-Frequency Capacitively Coupled Plasma* (MS thesis) (Dalian: Dalian University of Technology)

[24] Deng Y F, Han X W, Shafiq-ur Rehman and Liu Y 2008 *Phys. Plasmas* **15** 053507

[25] Bogaerts A 2004 *Spectrochim. Acta* B **9** 126

[26] Uchida Y, Takaki K, Urashima K and Chang J S 2004 *IEEEE Transacitions on Dielectrics and Electrial Insulation* **11** 491

[27] Gao F, Mao M, Ding Z F and Wang Y N 2008 *Acta Phys. Sin.* **57** 5123 (in Chinese)

[28] Wang Y H and Wang D Z 2003 *Acta Phys. Sin.* **52** 1694 (in Chinese)

[29] Brunet and Serra J Rocca 1984 *J. Appl. Phys.* **57** 1574